Arthritis & Rheumatology
Vol. 75, No. 5, May 2023, pp 768–781
DOI 10.1002/art.42394

American College of Rheumatology
Empowering Rheumatology Professionals

Identification of a Distinct Monocyte-Driven Signature in Systemic Sclerosis Using Biophysical Phenotyping of Circulating Immune Cells

Alexandru-Emil Matei,[1] Markéta Kubánková,[2] Liyan Xu,[1] Andrea-Hermina Györfi,[1] Evgenia Boxberger,[3] Despina Soteriou,[4] Maria Papava,[3] Julia Prater,[3] Xuezhi Hong,[1] Christina Bergmann,[3] Martin Kräter,[2] Georg Schett,[3] Jochen Guck,[2] and Jörg H. W. Distler[1]

Objective. Pathologically activated circulating immune cells, including monocytes, play major roles in systemic sclerosis (SSc). Their functional characterization can provide crucial information with direct clinical relevance. However, tools for the evaluation of pathologic immune cell activation and, in general, of clinical outcomes in SSc are scarce. Biophysical phenotyping (including characterization of cell mechanics and morphology) provides access to a novel, mostly unexplored layer of information regarding pathophysiologic immune cell activation. We hypothesized that the biophysical phenotyping of circulating immune cells, reflecting their pathologic activation, can be used as a clinical tool for the evaluation and risk stratification of patients with SSc.

Methods. We performed biophysical phenotyping of circulating immune cells by real-time fluorescence and deformability cytometry (RT-FDC) in 63 SSc patients, 59 rheumatoid arthritis (RA) patients, 28 antineutrophil cytoplasmic antibody–associated vasculitis (AAV) patients, and 22 age- and sex-matched healthy donors.

Results. We identified a specific signature of biophysical properties of circulating immune cells in SSc patients that was mainly driven by monocytes. Since it is absent in RA and AAV, this signature reflects an SSc-specific monocyte activation rather than general inflammation. The biophysical properties of monocytes indicate current disease activity, the extent of skin or lung fibrosis, and the severity of manifestations of microvascular damage, as well as the risk of disease progression in SSc patients.

Conclusion. Changes in the biophysical properties of circulating immune cells reflect their pathologic activation in SSc patients and are associated with clinical outcomes. As a high-throughput approach that requires minimal preparations, RT-FDC–based biophysical phenotyping of monocytes can serve as a tool for the evaluation and risk stratification of patients with SSc.

INTRODUCTION

Systemic sclerosis (SSc) is an autoimmune fibrotic disease of unknown etiology. SSc is associated with substantial morbidity and is one of the autoimmune diseases with the highest mortality (1). Key pathogenic hallmarks of SSc include autoimmunity, inflammation, fibrotic tissue remodeling, and microvascular damage. Dysregulated immune responses, involving both innate and

Presented by Dr. Matei in partial fulfillment of the requirements for a Dr. rer. biol. hum. degree, Friedrich-Alexander University Erlange-Nürnberg, Erlangen, Germany.

Dr. Matei's work was supported by the German Research Foundation (grant MA 9219/2-1), the Else Kröner-Fresenius-Foundation (grant 2021_EKEA.03), and the ELAN Foundation Erlangen (grant 19-12-06-1-Matei). Dr. Györfi's work was supported by the ELAN Foundation Erlangen (grant 21-07-23-1-Györfi). Dr. Schett's work was supported by the German Research Foundation (grant SFB CRC1181–261193037), and the German Federal Ministry of Education and Research MASCARA program TP 2 (grant 01EC1903A). Dr. Distler's work was supported by the German Research Foundation (grants DI 1537/14-1, DI 1537/17-1, DI 1537/20-1, DI 1537/22-1, and SFB CRC1181–261193037 [C01]), the Interdisciplinary Centre for Clinical Research (grant A64), the Else Kröner-Fresenius-Foundation (grant 2014_A47), the Wilhelm Sander Foundation (grant 2013.056.1), and the Ernst Jung Career Advancement Award for Medical Research from the Jung Foundation for Science and Research.

[1]Alexandru-Emil Matei, MD, Liyan Xu, MD, Andrea-Hermina Györfi, MD, Xuezhi Hong, MD, Jörg H. W. Distler, MD: Department of Rheumatology and Hiller Research Unit, University Hospital Düsseldorf, Medical Faculty of Heinrich Heine University, Düsseldorf, Germany, and Department of Internal Medicine 3–Rheumatology and Immunology and Deutsches Zentrum Immuntherapie (DZI), Friedrich-Alexander University Erlangen-Nürnberg (FAU), and Universitätsklinikum Erlangen, Erlangen, Germany; [2]Markéta Kubánková, PhD, Martin Kräter, PhD, Jochen Guck, PhD: Max Planck Institute for the Science of Light & Max-Planck-Center für Physik und Medizin, Erlangen, Germany, and Biotechnology Center, Center for Molecular and Cellular Bioengineering, Technische Universität Dresden, Dresden, Germany; [3]Evgenia Boxberger, MD, Maria Papava, MD, Julia Prater, MD, Christina Bergmann, MD, Georg Schett, MD: Department of Internal Medicine 3–Rheumatology and Immunology and Deutsches Zentrum Immuntherapie (DZI), Friedrich-Alexander-University Erlangen-Nürnberg (FAU) and Universitätsklinikum Erlangen, Erlangen, Germany; [4]Despina Soteriou, PhD: Max Planck Institute for the Science of Light & Max-Planck-Center für Physik und Medizin, Erlangen, Germany.

adaptive immunity, are major pathogenic players at the onset of SSc and are important drivers of disease progression (2).

Several circulating immune cell subsets (including T cells, B cells, natural killer [NK] cells, monocytes, and dendritic cells) have, beyond changed frequencies, an abnormal functional state in SSc (3–9). While the function of circulating cells can be characterized by their marker expression, few markers unambiguously identify distinct functional states of immune cells in SSc. A comprehensive functional profile of the circulating cells can only be obtained by complex, high-dimensional phenotyping with methods such as single-cell RNA sequencing or mass cytometry, or by functional assays (10). However, these approaches are expensive and time-consuming and thus cannot be used for high-throughput testing as part of routine clinical assessment.

While the relevance of biochemical properties for cell physiology is well-established, biophysical properties of cells such as morphology and mechanics are just beginning to emerge as markers of cell function (11–13). Biophysical properties have been shown to indicate distinct stages in stem cell differentiation or distinct leukocyte activation states (14–16). Moreover, changes in the biophysical properties of leukocyte subsets are intrinsically linked with pathophysiologic processes such as margination, extravasation, infiltration in the target tissue, and migration toward chemoattractants (17,18). For example, leukocyte stiffening might be necessary for retention in capillaries, whereas softening might be required for extravasation (19).

Pathologic changes in the biophysical properties of circulating immune cells have recently been described in the setting of several infectious diseases, such as malaria and viral respiratory tract infections, including COVID-19, as well as in hematologic-oncologic diseases such as acute lymphoid and myeloid leukemia, or malignant pleural effusions (20–22). However, biophysical profiling of circulating leukocytes has not been performed in autoimmune rheumatic diseases so far.

Real-time fluorescence and deformability cytometry (RT-FDC) is a novel technique that enables simultaneous assessment of multiple physical parameters of individual cells, such as deformation under shear stress, Young's modulus (a measure of cell stiffness), and cell size, in a high-throughput manner (23,24). These parameters are derived from brightfield images of cells acquired as they flow through a channel constriction in a microfluidic chip. As the RT-FDC device can also detect fluorescent signals, fluorescence immunolabeling enables the identification of major leukocyte subpopulations by marker expression and their in-depth physical characteristics. Of particular note, RT-FDC measurements can be performed with a throughput of up to 1,000 cells per second, which enables characterization of rare leukocyte subsets and measurements of multiple samples in the same day (25). Moreover, RT-FDC measurements require only minimal cell preparations or specific reagents (26), further facilitating high-throughput analyses at low costs. Therefore, biophysical phenotyping of circulating leukocytes using RT-FDC could potentially be applied in disease diagnostics and in routine clinical follow-up.

We hypothesized that aberrant immune cell activation in SSc might be accompanied by changes in the biophysical properties of these cells, and that these changes, in turn, might reflect disease activity, severity, or progression. Therefore, we performed RT-FDC–based biophysical phenotyping of the most frequent subpopulations of circulating leukocytes in patients with SSc.

Here, we describe changes in the biophysical properties of several leukocyte subpopulations in SSc patients, many of which are specific to SSc rather than general reflections of inflammation, as they are not observed in patients with rheumatoid arthritis (RA) or antineutrophil cytoplasmic antibody–associated vasculitis (AAV). Biophysical alterations of monocyte subsets are not only associated with current disease activity, manifestations of microvascular damage, and the extent of fibrosis, but also with future risk of disease progression in SSc patients. The changes in biophysical properties of circulating monocytes in SSc patients can be partially reproduced in vitro by exposure of healthy monocytes to transforming growth factor β (TGFβ) or to serum from SSc patients, suggesting that a profibrotic environment might be responsible in part for these changes. Although further studies are required, our results provide the first evidence that biophysical phenotyping of circulating leukocytes may offer diagnostic potential in SSc.

PATIENTS AND METHODS

We performed RT-FDC measurements of peripheral blood mononuclear cells (PBMCs) isolated from 22 healthy controls, 63 patients with SSc, 59 patients with RA, and 28 patients with AAV after immunolabeling to identify major circulating immune cells and characterize their biophysical phenotype. Measurements were performed between May 2019 and October 2021. Demographic data from all study groups (SSc patients, RA patients, AAV patients, and healthy controls) are summarized in Supplementary Table 1, available on the *Arthritis & Rheumatology* website at http://onlinelibrary.wiley.com/doi/10.1002/art.42394. We included donors ages >18 years who fulfilled the respective classification criteria for SSc, RA, or AAV without further inclusion criteria, in the order of their visit in the outpatient department, without randomization. We excluded patients with overlap of SSc, RA, or AAV with other rheumatologic diseases, including other connective tissue diseases or sarcoidosis and patients with

Author disclosures are available at https://onlinelibrary.wiley.com/action/downloadSupplement?doi=10.1002%2Fart.42394&file=art42394-sup-0001-Disclosureform.pdf.

Address correspondence via email to Alexandru-Emil Matei, MD, at alexandru-emil.matei@med.uni-duesseldorf.de.

Submitted for publication February 2, 2022; accepted in revised form October 18, 2022.

active infection or malignant tumors. The researchers performing the measurements (AEM, MK, LX) were blinded with regard to diagnosis and clinical data. Additional descriptions of the materials and methods used in this study are available on the *Arthritis & Rheumatology* website at http://onlinelibrary.wiley.com/doi/10.1002/art.42394.

Data availability. All data generated or analyzed during this study are included in this published article (and its Supplementary files). Additional supporting information or raw data are available as deidentified participant data sets from the corresponding author upon request.

RESULTS

Study design and RT-FDC measurements. We first aimed to analyze whether circulating leukocytes in SSc patients have specific biophysical properties that distinguish them from the leukocytes of healthy donors or patients with other autoimmune rheumatic diseases such as RA and AAV. For this, we collected peripheral blood samples from 63 SSc patients, 59 RA patients, 28 AAV patients, and 22 healthy controls, isolated and immunolabeled PBMCs, and performed RT-FDC measurements (Figures 1A–C).

To identify the major subpopulations of leukocytes in heterogeneous PBMC samples, we designed 5 antibody panels, each consisting of a combination of 3 surface markers, to identify the major subpopulations of lymphoid cells (T helper cells, T cytotoxic cells, B cells, NK cells, and natural killer T [NKT]–like cells) and myeloid cells (classical, intermediate, and inflammatory monocytes, type 2 conventional dendritic [cDC2] cells, and plasmacytoid dendritic [pDCs] cells) by standard gating strategies used in flow cytometry (Figure 1D and Supplementary Figure 1, http://onlinelibrary.wiley.com/doi/10.1002/art.42394) (27–29). Using this strategy, we were able to analyze the following biophysical properties of single cells from each subpopulation: 1) cross-sectional area (as a measurement of cell size), 2) deformation (i.e., deviation from a perfect circle due to shear stresses in a cell flowing through a constriction in the microfluidic chip), and 3) Young's modulus (i.e., a measurement of cell stiffness). Cell deformation is correlated with cell area; bigger cells are subjected to higher shear stresses than smaller cells with identical stiffness and thus deform more. Young's modulus is independent of cell size and is used as a parameter of cell stiffness.

Starting from the single-cell data, we calculated the median and SD of the biophysical parameters of all cells belonging to 1 population from 1 donor (i.e., intra-donor median [$median_{ID}$] and intra-donor SD [SD_{ID}] of area, deformation, and Young's modulus) and evaluated changes in these parameters in SSc, RA, and AAV patients compared to healthy controls. We also evaluated the associations of these parameters with clinical parameters in SSc patients (Figure 1E). The biophysical properties of all PBMC populations from healthy donors are summarized in Supplementary Table 6 (http://onlinelibrary.wiley.com/doi/10.1002/art.42394).

SSc-specific changes in biophysical properties of circulating monocytes, NK cells, and NKT-like cells. We evaluated in an exploratory, unbiased manner whether the biophysical properties of individual leukocyte subpopulations differ between SSc patients and matched healthy individuals or patients with RA or AAV. We observed a consistent pattern of changes in the biophysical properties of lymphoid cell subpopulations in patients with SSc compared to the other groups, with significantly higher $median_{ID}$ of cross-sectional areas of CD4+ and CD8+ T cells, NK cells, and NKT-like cells (Figures 2A–C and Supplementary Figures 2A and B, http://onlinelibrary.wiley.com/doi/10.1002/art.42394). Among myeloid cells, classical and intermediate monocytes had a significantly higher SD_{ID} of deformation in SSc patients compared to healthy donors, whereas inflammatory monocytes had a higher $median_{ID}$ of deformation (Figures 2D–F and Supplementary Figures 2C–E). The change in SD_{ID} suggests intra-donor changes in deformation of subpopulations of these cells (e.g., as a consequence of activation, rather than a shift in the deformation of the whole population). Of note, B cells, cDC2 cells, and pDCs had comparable properties in SSc patients and healthy controls, suggesting that changes in the biophysical properties of leukocytes in SSc patients are cell population–specific (Figure 2A).

In SSc patients, the pattern of changes in the biophysical properties of circulating leukocytes was strikingly different compared to that in RA patients, AAV patients, and healthy controls (Supplementary Figures 3A and 4A, http://onlinelibrary.wiley.com/doi/10.1002/art.42394). Most changes observed in SSc patients were SSc-specific; NK cells and NKT-like cells had a higher $median_{ID}$ of cross-sectional area, classical and intermediate monocyte subsets had a higher SD_{ID} of deformation, and inflammatory monocytes had a higher $median_{ID}$ of deformation in SSc patients compared to healthy controls, RA patients, and AAV patients (Supplementary Figures 3B–F and 4B–F). However, some of the changes were shared between RA, AAV, and SSc patients. For instance, CD4+ and CD8+ T cells had a higher $median_{ID}$ of cross-sectional area in SSc, RA, and AAV patients compared to healthy controls (Supplementary Figures 3G and H and 4G and H). For further analyses, we focused on the leukocyte subpopulations with SSc-specific changes in their biophysical properties.

Correlation of biophysical properties of monocytes with disease activity in SSc. We next evaluated whether the biophysical properties of circulating leukocytes were associated with disease activity in SSc patients (assessed by the European Scleroderma Trials and Research [EUSTAR] activity index) (30). In particular, the biophysical properties of monocyte subsets were changed in patients with active disease; classical and intermediate

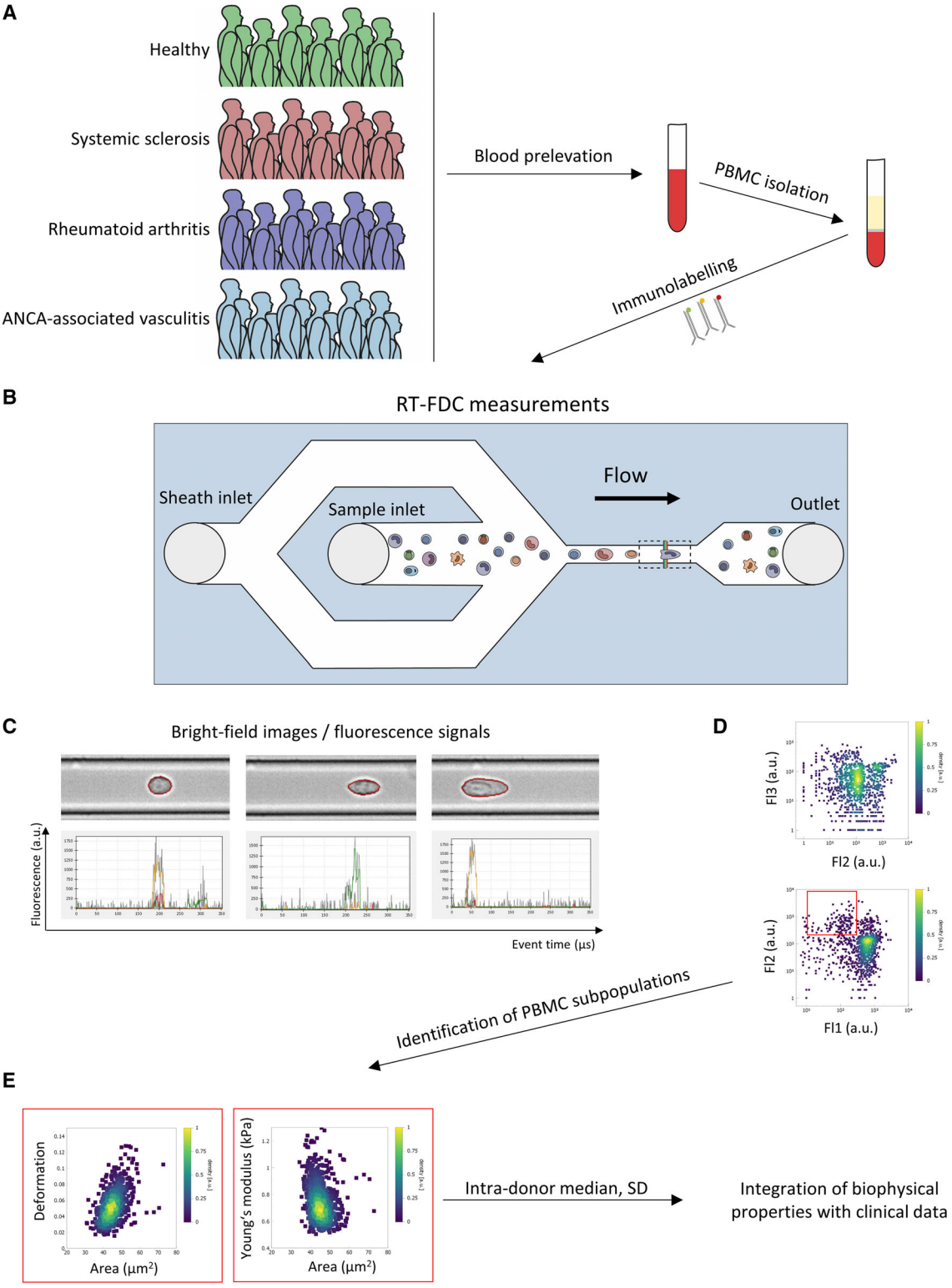

Figure 1. Design of the current study on the association of biophysical properties of circulating immune cells and their pathologic activation in systemic sclerosis (SSc) patients. **A**, Schematic representation of the study design including the study cohort and immunolabeling of participant peripheral blood mononuclear cells (PBMCs). **B** and **C**, Schematic representation of the deformation of cells moving through a constriction channel in a microfluidic chip (**B**) and subsequent representative brightfield images of cells of different cross-sectional area and deformation (contours in red) (**C**) acquired at a region (dashed rectangle in **B**) in which 3 lasers excited fluorophores on the antibodies bound to cell surface markers (corresponding fluorescence signals in bottom row of **C**). **D** and **E**, Representative scatter plots of fluorescence signal intensities, illustrating the approach for identification of leukocyte subpopulations by gating according to marker expression (**D**) and of area, deformation, and Young's modulus of individual cells (**E**). ANCA = antineutrophil cytoplasmic antibody; RT-FDC = real-time fluorescence and deformability cytometry.

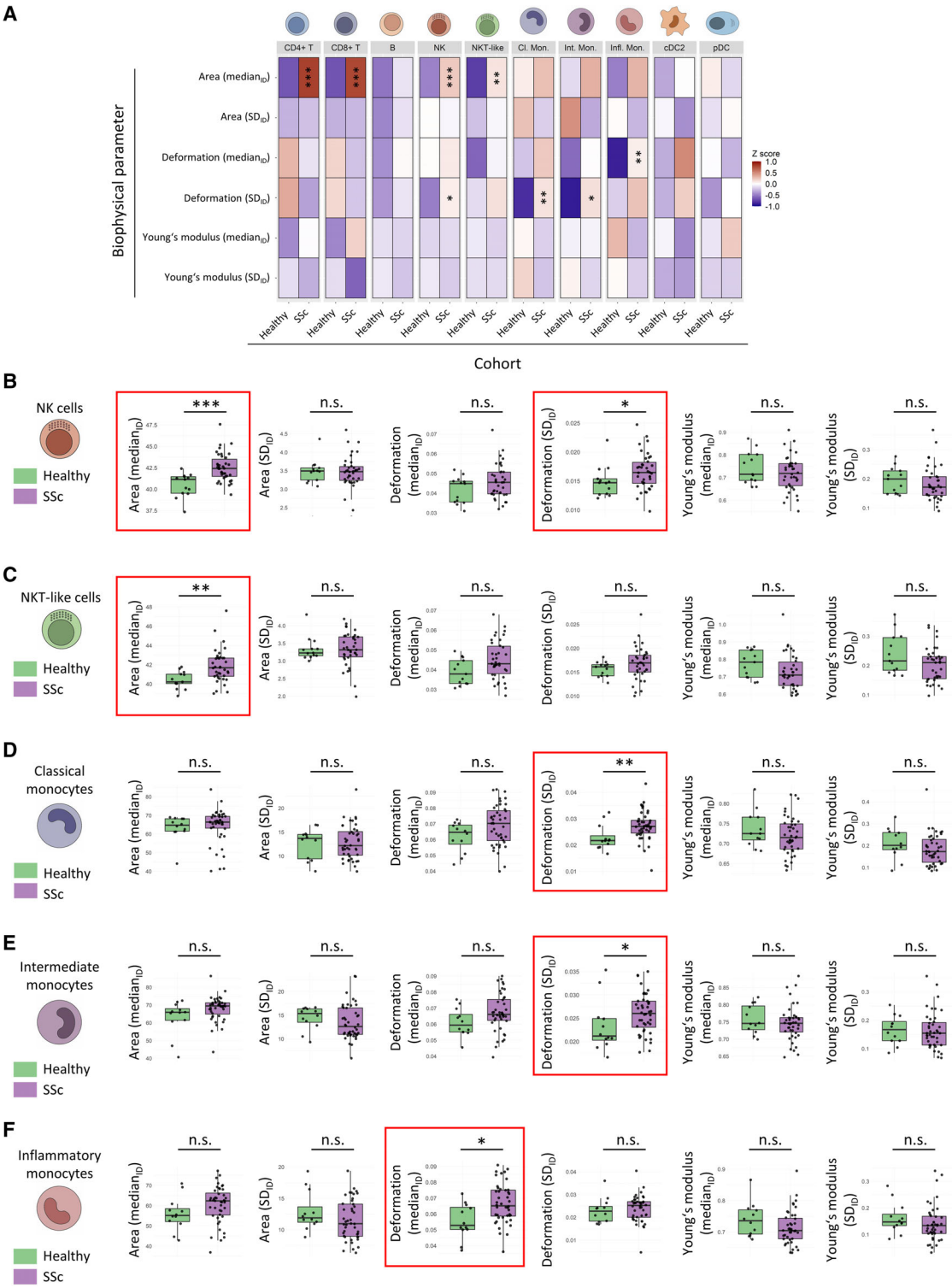

Figure 2. Changes in biophysical properties of immune cell subpopulations in systemic sclerosis (SSc) patients. **A**, Heatmap of normalized biophysical parameters of immune cell subpopulations. **B–F**, Box plots showing the intra-donor median (median$_{ID}$) and intra-donor SD (SD$_{ID}$) of area, deformation, and Young's modulus of cell populations with SSc-specific differences (distinct biophysical parameters in SSc patients compared to healthy donors, but not in rheumatoid arthritis or antineutrophil cytoplasmic antibody–associated vasculitis patients compared to healthy donors). Each circle represents the median$_{ID}$ or SD$_{ID}$ of all cells in the indicated immune cell subpopulation from 1 donor. Lines inside the boxes represent the median. Boxes represent the 25th to 75th percentiles. Lines outside the boxes represent the 10th and 90th percentile. * $P < 0.05$; ** = $P < 0.01$; *** = $P < 0.001$ by Mann-Whitney U test with Hochberg's correction for multiple testing (red frames indicate significant differences). NK = natural killer; NKT-like = natural killer T–like; Cl. Mon. = classical monocyte; Int. Mon. = intermediate monocyte; Infl. Mon. = inflammatory monocyte; cDC2 = type 2 conventional dendritic cell; pDC = plasmacytoid dendritic cell; n.s. = not significant.

monocytes had a lower SD_{ID} of cross-sectional area, intermediate and inflammatory monocytes had a higher $median_{ID}$ of deformation, and intermediate monocytes also had a higher $median_{ID}$ of cross-sectional area in patients with active SSc compared to patients with stable disease (Figures 3A–D and Supplementary Figure 5, http://onlinelibrary.wiley.com/doi/10.1002/art.42394).

In SSc patients, the odds of having active disease decreased with higher SD_{ID} of cross-sectional area of classical and intermediate monocytes and increased with higher $median_{ID}$ of deformation of intermediate and inflammatory monocytes both in simple logistic regression models and after adjustment for antibody status, immunosuppressive therapy, diffuse or limited skin involvement (with diffuse skin involvement as independent predictor), diffusing capacity for carbon monoxide (DL_{CO}), monocyte counts, or donor age (Supplementary Table 7, http://onlinelibrary.wiley.com/doi/10.1002/art.42394). The SD_{ID} of cross-sectional area of classical and intermediate monocytes also negatively correlated with the EUSTAR index as a continuous variable (Figures 3E–G). Moreover, the $median_{ID}$ of cross-sectional area of classical and intermediate monocytes correlated positively with the EUSTAR activity index, whereas the SD_{ID} of the Young's modulus of classical monocytes correlated negatively with the EUSTAR activity index (Figures 3E–G).

Indication of the severity of dermal fibrosis in SSc by the biophysical properties of monocytes. We next analyzed potential correlations between the biophysical properties of circulating leukocytes and the severity of skin involvement in SSc patients. Classical and intermediate monocytes had a lower SD_{ID} of cross-sectional area in patients with diffuse cutaneous SSc (dcSSc) compared to patients with limited cutaneous SSc (lcSSc) and healthy controls (Figures 4A–C and Supplementary Figures 6A and B, http://onlinelibrary.wiley.com/doi/10.1002/art.42394). Classical monocytes also had a higher $median_{ID}$ of deformation and a lower SD_{ID} of Young's modulus in dcSSc patients compared to lcSSc patients and healthy controls (Figures 4A and B and Supplementary Figure 6A). The odds of having diffuse skin involvement decreased with higher SD_{ID} of cross-sectional area of classical and intermediate monocytes and with higher SD_{ID} of Young's modulus of classical monocytes, both in simple logistic regression models and after adjustment for antibody status, immunosuppressive therapy, monocyte counts, and donor age (Supplementary Table 8, http://onlinelibrary.wiley.com/doi/10.1002/art.42394).

The $median_{ID}$ of cross-sectional area and the $median_{ID}$ of deformation of all monocyte subpopulations positively correlated with the modified Rodnan skin thickness score (MRSS) (31), whereas the SD_{ID} of area, deformation, and Young's modulus of classical monocytes and the SD_{ID} of cross-sectional area in intermediate monocytes negatively correlated with the MRSS (Figure 4D and Supplementary Figures 6D–F, http://onlinelibrary.wiley.com/doi/10.1002/art.42394).

The SD_{ID} of deformation for all monocyte subsets was significantly lower in patients with progression of skin involvement at the time of measurement as compared to skin involvement observed at a previous visit (6 months earlier) (Supplementary Figure 7 and Supplementary Table 9, http://onlinelibrary.wiley.com/doi/10.1002/art.42394). This further highlights that biophysical phenotyping of monocyte subsets can indicate the severity of skin involvement in SSc patients.

Reflection of the severity of pulmonary fibrosis in SSc by the biophysical properties of monocytes. We next evaluated whether the biophysical properties of circulating leukocytes can indicate the severity of lung involvement in SSc patients. In general, monocyte subsets had a lower SD_{ID} of cross-sectional area and deformation, and classical monocytes also had a lower SD_{ID} of Young's modulus in patients with extensive interstitial lung disease (ILD) (defined according to Goh et al) (32) compared to patients without ILD or with limited ILD (Figures 5A–D and Supplementary Figure 8, http://onlinelibrary.wiley.com/doi/10.1002/art.42394). In SSc patients, the odds of having extensive ILD (relative to the odds of having limited or no ILD) decreased with higher SD_{ID} of deformation in all monocyte subsets both in simple logistic regression models and when adjusting for antibody status, immunosuppressive therapy, diffuse or limited skin involvement, activity status, monocyte counts, and donor age (Supplementary Table 10, http://onlinelibrary.wiley.com/doi/10.1002/art.42394). In SSc patients without confirmed pulmonary hypertension, SD_{ID} of cross-sectional area in intermediate and inflammatory monocytes positively correlated with the DL_{CO}, whereas SD_{ID} of deformation in all monocyte subsets showed a trend toward positive correlation, suggesting that, in patients with SSc-related ILD (SSc-ILD), worsening of lung function is associated with a more compact intra-donor distribution of area and deformation of monocyte subsets (Figures 5E–G).

In patients with progression of SSc-ILD at the time of measurement as compared to measurements taken during a previous visit (1 year earlier), assessed according to the definition from the INBUILD trial (33), classical and intermediate monocytes had a lower SD_{ID} of deformation, whereas all monocyte subsets had a higher $median_{ID}$ of Young's modulus than patients with stable lung involvement (Figures 6A–F and Supplementary Table 11, http://onlinelibrary.wiley.com/doi/10.1002/art.42394). Furthermore, SD_{ID} of deformation in inflammatory monocytes positively correlated with the change in forced vital capacity (FVC) at the time of measurement as compared to a visit 1 year prior (ΔFVC; Figures 6G and H). We also observed a positive correlation trend between the SD_{ID} of deformation in the other monocyte subsets and a negative correlation trend between Young's modulus of all monocyte subsets and ΔFVC, suggesting that, in patients with worsening lung function, all monocyte subsets might have a more compact distribution of deformation and might be stiffer (Figure 6G).

The odds of having progressive ILD at the time of measurement decreased with a higher SD_{ID} of deformation in classical and intermediate monocytes and increased with a higher

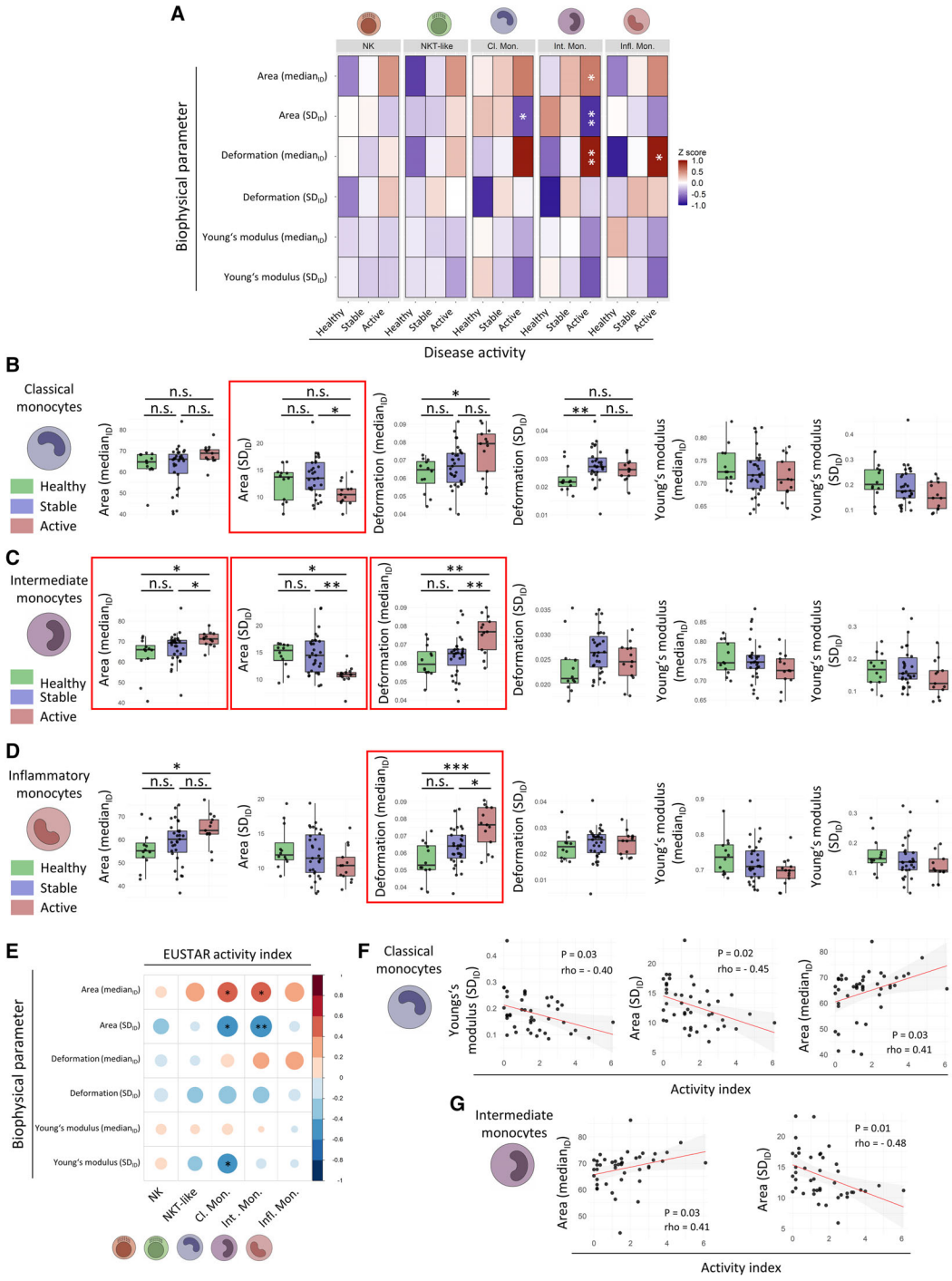

Figure 3. Biophysical properties of monocyte subsets in SSc patients stratified by disease activity. **A**, Heatmap of the normalized biophysical parameters of immune cell subpopulations with SSc-specific changes according to SSc-specific disease activity levels. **B–D**, Box plots illustrating the biophysical parameters (median$_{ID}$ or SD$_{ID}$ of area, deformation, and Young's modulus) of classical (**B**), intermediate (**C**), and inflammatory monocytes (**D**) in patients with active SSc as compared to patients with stable SSc and healthy donors. Each circle represents the median$_{ID}$ or SD$_{ID}$ of all cells in the indicated immune cell subpopulation from 1 donor. Lines inside the boxes represent the median. Boxes represent the 25th to 75th percentiles. Lines outside the boxes represent the 10th and 90th percentile. Significant differences are highlighted with red frames. **E**, Correlogram illustrating the Spearman's correlation between the European Scleroderma Trials and Research Group (EUSTAR) activity index and the biophysical properties of immune cell subpopulations with SSc-specific changes. **F–G**, Scatter plots illustrating statistically significant correlations between EUSTAR activity index score and biophysical properties of classical monocytes (**F**) and intermediate monocytes (**G**). In **F** and **G**, each circle corresponds to the median$_{ID}$ or SD$_{ID}$ of the respective parameter (median or SD of all the cells belonging to the respective subpopulation from 1 donor). * $P < 0.05$; ** = $P < 0.01$; *** = $P < 0.001$ by Dunn's post-hoc test with Hochberg's correction for multiple testing (**A**–**D**) or by Spearman's 2-sided test with Hochberg's correction for multiple testing (**E**–**G**). See Figure 2 for definitions.

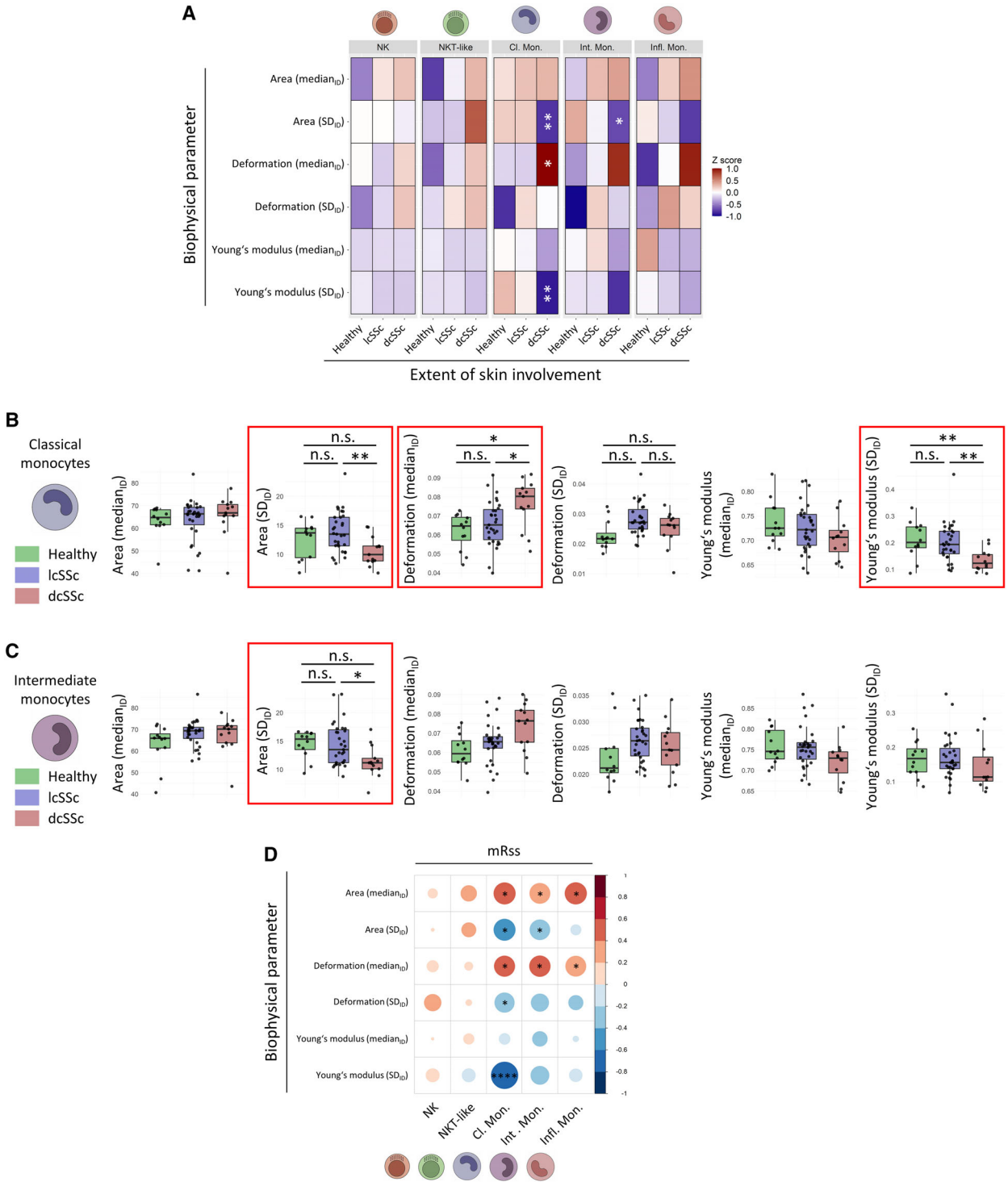

Figure 4. Biophysical properties of monocyte subsets indicate the severity of skin fibrosis in SSc. **A**, Heatmap of the normalized biophysical parameters of immune cell subpopulations according to SSc patient groups stratified by the extent of skin involvement, including patients with limited cutaneous SSc (lcSSc) or diffuse cutaneous SSc (dcSSc) and healthy donors. **B–C**, Box plots illustrating the biophysical parameters (median$_{ID}$ or SD$_{ID}$ of area, deformation, or Young's modulus) of classical (**B**) and intermediate (**C**) monocytes in patients with dcSSc, lcSSc, and healthy donors. Each circle represents the median$_{ID}$ or SD$_{ID}$ of all cells in the indicated immune cell subpopulation from 1 donor. Lines inside the boxes represent the median. Boxes represent the 25th to 75th percentiles. Lines outside the boxes represent the 10th and 90th percentile. Significant differences are highlighted with red frames. **D**, Correlogram illustrating the Spearman's correlation between modified Rodnan skin thickness score (mRss) and the biophysical properties of immune cells subpopulations (with SSc-specific changes). * $P < 0.05$; ** $= P < 0.01$; **** $= P < 0.0001$ by Dunn's post-hoc test with Hochberg's correction for multiple testing (**A–C**) or by Spearman's 2-sided test with Hochberg's correction for multiple testing (**D**). See Figure 2 for definitions. Color figure can be viewed in the online issue, which is available at http://onlinelibrary.wiley.com/doi/10.1002/art.42394/abstract.

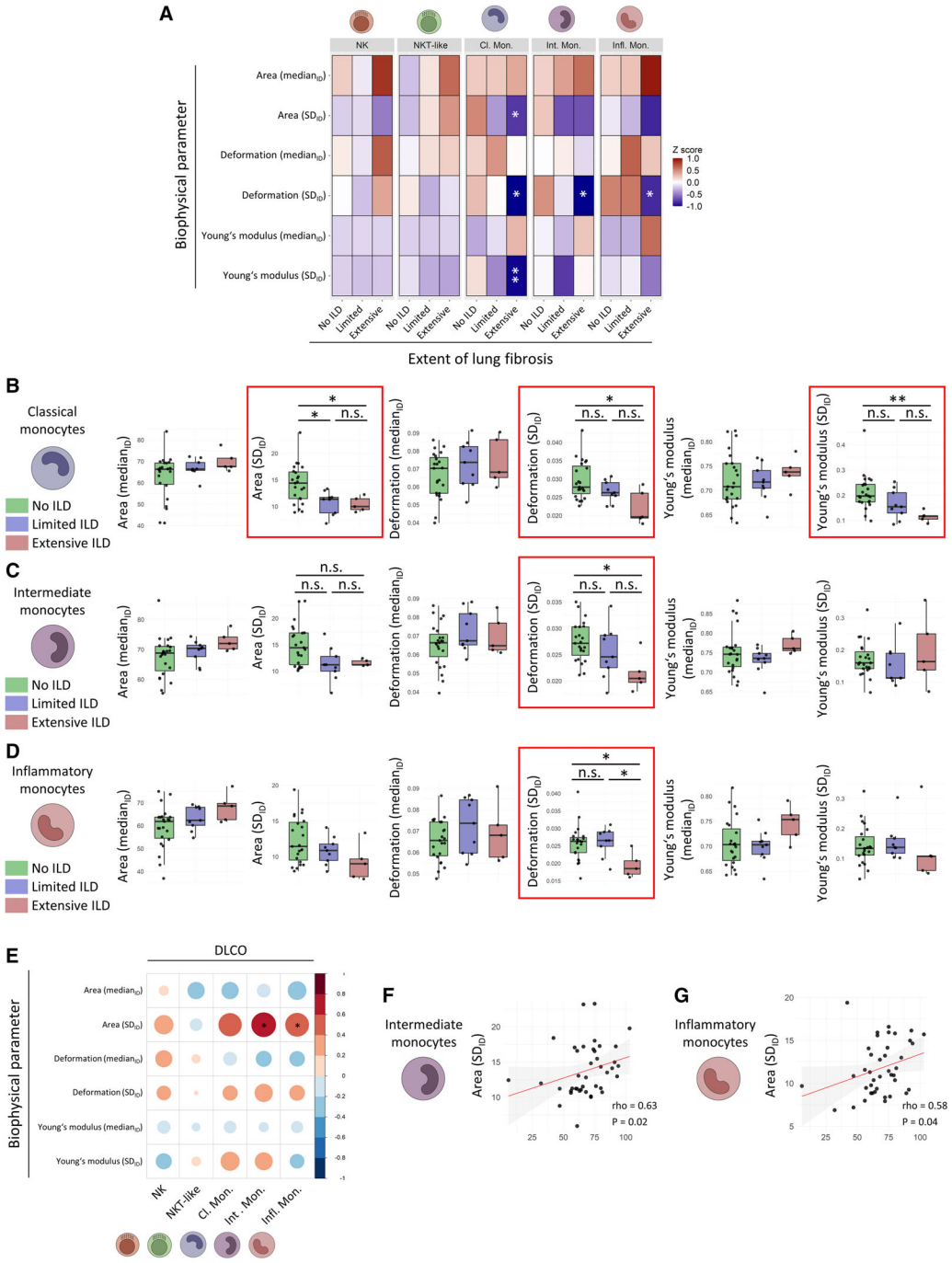

Figure 5. Biophysical properties of monocyte subsets associated with severity of SSc-related interstitial lung disease (SSc-ILD). **A**, Heatmap of normalized biophysical parameters of immune cell subpopulations according to SSc-specific changes in the extent of lung fibrosis in patients with limited or extensive SSc-ILD and those with no ILD. **B–D**, Box plots illustrating the biophysical parameters (median$_{ID}$ or SD$_{ID}$ of area, deformation, and Young's modulus) of classical (**B**), intermediate (**C**), and inflammatory (**D**) monocytes in patients with limited or extensive SSc-ILD compared to patients without SSc-ILD. Each circle represents the median$_{ID}$ or SD$_{ID}$ of all cells in the indicated immune cell subpopulation from 1 donor. Lines inside the boxes represent the median. Boxes represent the 25th to 75th percentiles. Lines outside the boxes represent the 10th and 90th percentile. Significant differences are highlighted with red frames. **E**, Correlogram illustrating Spearman's correlations between diffusing capacity for carbon monoxide (DL$_{CO}$) (in patients without diagnosed pulmonary hypertension [PH]) and the biophysical properties of immune cells with SSc-specific changes. **F** and **G**, Scatter plots illustrating statistically significant correlations between DL$_{CO}$ (in patients without diagnosed PH) and SD$_{ID}$ of cross-sectional area of intermediate monocytes (**F**) and inflammatory monocytes (**G**). In **F** and **G**, each circle corresponds to the median$_{ID}$ or SD$_{ID}$ of the respective parameter (median or SD of all the cells belonging to the respective subpopulation from 1 donor). * $P < 0.05$; ** = $P < 0.01$ by Dunn's post-hoc test with Hochberg's correction for multiple testing (**A–D**) or by Spearman's 2-sided test with Hochberg's correction for multiple testing (**E–G**). See Figure 2 for definitions.

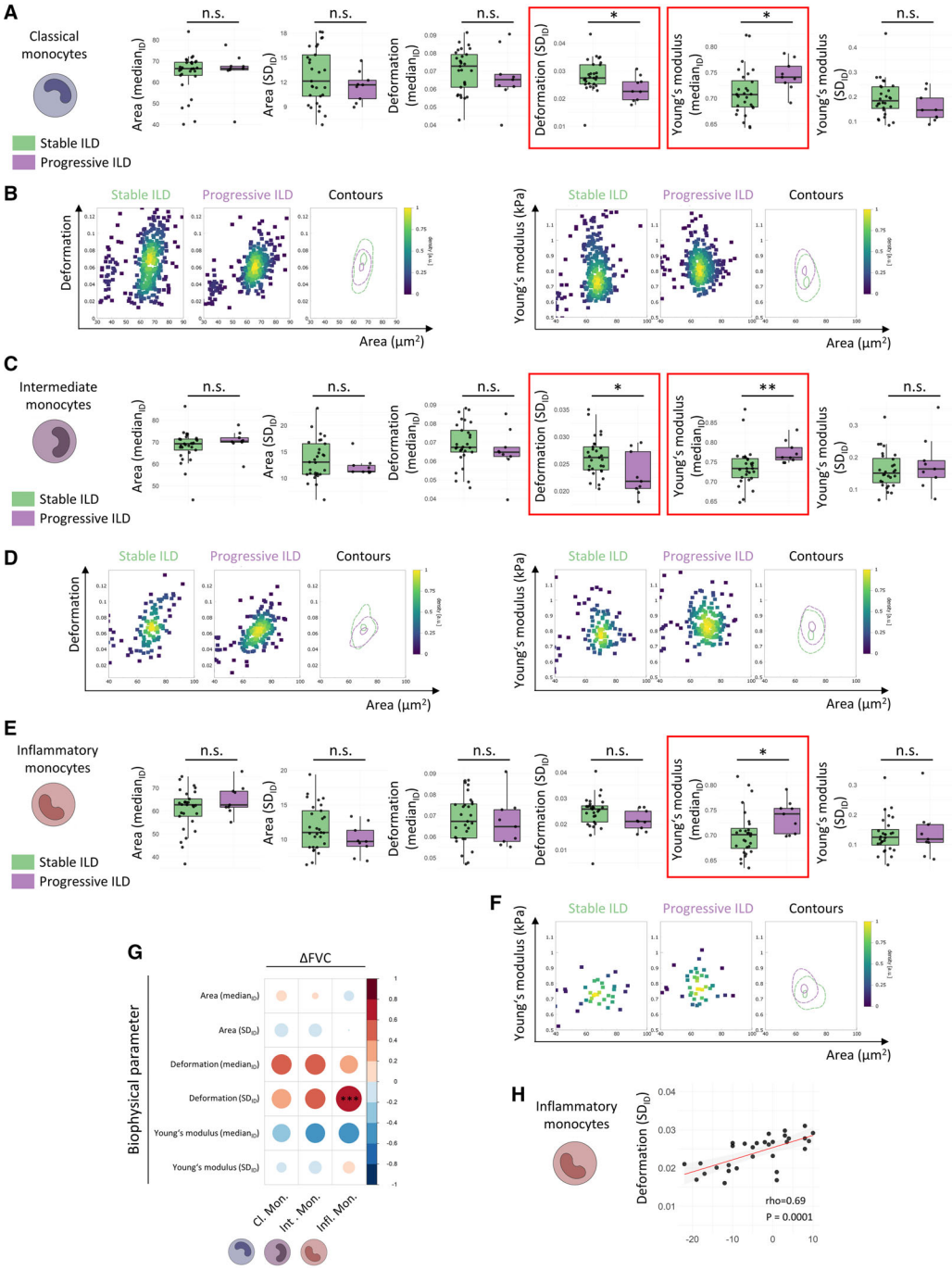

Figure 6. Biophysical properties of monocyte subsets indicate progression of SSc-related interstitial lung disease (SSc-ILD). **A**–**F**, Box plots illustrate the biophysical parameters (intra-donor median [median$_{ID}$]or intra-donor SD [SD$_{ID}$] of area, deformation, or Young's modulus) of classical (**A**), intermediate (**C**), and inflammatory (**E**) monocytes in patients with SSc-ILD progression in the year prior to the measurement compared to patients with stable SSc-ILD. Each circle represents the median$_{ID}$ or SD$_{ID}$ of all cells in the indicated immune cell subpopulation from 1 donor. Lines inside the boxes represent the median. Boxes represent the 25th to 75th percentiles. Lines outside the boxes represent the 10th and 90th percentile. Representative scatter plots and contour plots illustrate the intra-donor distribution of cross-sectional area, deformation, and Young's modulus of single classical (**B**), intermediate (**D**), and inflammatory (**F**) monocytes. Significant differences are highlighted with red frames. **G**, Correlogram illustrating Spearman's correlations between change in forced vital capacity (ΔFVC) at the time of measurement compared to 12 months earlier and the biophysical properties of monocyte subsets. **H**, Scatter plot illustrating the correlation between ΔFVC and SD$_{ID}$ of deformation of inflammatory monocytes. In **A**, **C**, **E,** and **H**, each circle corresponds to the median$_{ID}$ or SD$_{ID}$ of the respective parameter (median or SD of all the cells belonging to the respective subpopulation from 1 donor). * $P < 0.05$; ** = $P < 0.01$; *** = $P < 0.001$ by Mann-Whitney U test with Hochberg's correction for multiple testing (**A**, **C**, and **E**) or by Spearman's 2-sided test with Hochberg's correction for multiple testing (**G** and **H**). See Figure 2 for definitions.

median$_{ID}$ of Young's modulus of all monocyte subsets both in simple logistic regression models and when adjusting for antibody status, immunosuppressive therapy, diffuse or limited skin involvement, activity status, extensive or limited ILD (with extensive ILD as independent predictor), monocyte counts, and donor age (Supplementary Table 12, http://onlinelibrary.wiley.com/doi/10.1002/art.42394).

For a subset of patients with follow-up visits 1 year after the initial measurements, we also evaluated whether the mechanical properties of monocytes at baseline might predict future lung progression. The biophysical properties of intermediate monocytes were changed in patients who would go on to experience progression of SSc-ILD; the medianID of area was significantly higher and SD$_{ID}$ of deformation was lower (Supplementary Table 13, http://onlinelibrary.wiley.com/doi/10.1002/art.42394). Thus, changes in the biophysical properties of monocyte subsets can indicate the severity and might predict the progression of lung involvement in SSc patients.

Association of changes in biophysical properties of monocytes with clinical manifestations of microvascular damage in SSc. We further analyzed whether the biophysical properties of circulating immune cells were changed in SSc patients with clinical manifestations of microvascular damage as exemplified by pulmonary arterial hypertension (PAH) and active digital ulcerations. In patients with active digital ulcerations, inflammatory monocytes had a higher median$_{ID}$ of cross-sectional area (Supplementary Table 14, http://onlinelibrary.wiley.com/doi/10.1002/art.42394). In patients with PAH, classical monocytes had a lower SD$_{ID}$ of deformation, whereas intermediate monocytes had a higher median$_{ID}$ of Young's modulus (Supplementary Table 15, http://onlinelibrary.wiley.com/doi/10.1002/art.42394).

Reproducibility of RT-FDC–based biophysical phenotyping of circulating monocytes. We further aimed to evaluate the reproducibility of the RT-FDC measurements for determination of the biophysical properties of circulating monocytes. For this, we performed 2 repeated RT-FDC measurements of monocytes from the same donor and a PBMC isolation procedure on the same day for 9 healthy donors. We observed a high degree of overlap between the distributions of cross-sectional area, deformation, and Young's modulus of monocytes between the repeated measurements from the same donor for all 9 donors (Supplementary Figure 9A, http://onlinelibrary.wiley.com/doi/10.1002/art.42394).

One-way analysis of variance fitted on measurements from different donors as experimental groups and measurements from the same donor as replicates showed significant differences between donors for all RT-FDC parameters of monocytes, further demonstrating that RT-FDC measurements can capture the inter-donor variation in the biophysical properties of monocytes. The inter-donor variability accounted for a minimum of 76% (for the SD$_{ID}$ of Young's modulus) to a maximum of 95% (for median$_{ID}$ of Young's modulus) of the total (inter- and intra-donor) variability of the biophysical properties of monocytes (Supplementary Figure 9B, http://onlinelibrary.wiley.com/doi/10.1002/art.42394). These results demonstrate that RT-FDC measurements enable the reproducible characterization of the biophysical properties of circulating monocytes with minimal technical variability.

Changes in biophysical properties of monocytes in SSc patients partially reproduced in vitro by exposure of healthy monocytes to TGFβ or SSc serum. We next evaluated whether the changes in biophysical properties of monocytes observed in different subgroups of SSc patients could be reproduced in vitro by exposure of healthy monocytes to proinflammatory or profibrotic cytokines or to serum from SSc patients (Supplementary Figures 10A, B, and D, http://onlinelibrary.wiley.com/doi/10.1002/art.42394). Treatment with TGFβ, a key profibrotic mediator, induced an increase in median$_{ID}$ of Young's modulus of monocytes, whereas treatment with interleukin-6 (IL-6), a proinflammatory cytokine with central roles in autoimmunity, did not induce significant changes in the biophysical properties of monocytes (Supplementary Figures 10C and 11A and B, http://onlinelibrary.wiley.com/doi/10.1002/art.42394) (34,35). Exposure to pooled serum from SSc patients with anti–topoisomerase I antibody positivity, with active disease, and with extensive, progressive ILD, induced an increase in median$_{ID}$ of Young's modulus and a decrease in SD$_{ID}$ of deformation of monocytes, whereas exposure to pooled serum from SSc patients with anticentromere antibody positivity, with stable disease, and without ILD did not induce significant changes in the biophysical properties of monocytes (with exposure to autologous serum as control).

Of note, similar changes in the biophysical properties of monocytes from healthy donors exposed in vitro to TGFβ or SSc patient serum were observed in circulating monocytes of different subsets of SSc patients. Circulating monocytes from patients with progressive ILD had a higher median$_{ID}$ of Young's modulus in comparison to patients with stable ILD (Figures 6A–F), which is a change that can be induced in cultured healthy monocytes by exposure to either TGFβ or serum from SSc patients with progressive ILD (Supplementary Figures 10C and E, and 11B and D, http://onlinelibrary.wiley.com/doi/10.1002/art.42394). Moreover, circulating monocytes from patients with extensive and/or progressive ILD had a lower SD$_{ID}$ of deformation (Figures 5A–D and 6A–F and Supplementary Figure 8, http://onlinelibrary.wiley.com/doi/10.1002/art.42394), and this change can be induced in cultured healthy monocytes by exposure to serum from SSc patients with extensive, progressive ILD (Supplementary Figures 10C and E, and 11B and D).

DISCUSSION

In this study, we demonstrated that RT-FDC can detect changes in the biophysical properties of individual immune cell

populations in SSc patients with high reproducibility. In general, lymphoid subsets (except for B cells) had a higher cross-sectional area in SSc patients compared to healthy controls, whereas myeloid cells had a higher intra-donor heterogeneity in their distribution of deformation in SSc patients compared to healthy controls. Moreover, we demonstrated that most of these changes were specific to patients with SSc and were not observed in patients with RA or AAV, indicating that they were not merely a reflection of inflammatory or autoimmune activity, but rather reflect disease-specific changes. Consistent with this conclusion, biophysical changes of monocyte subsets are associated with clinical features of SSc, such as disease activity and the severity of skin and lung involvement, independently of other features, such as autoantibody status, immunosuppressive therapy, donor age, or monocyte counts (where high monocyte counts are a biomarker of poor outcomes in fibrosis) (36), and might identify patients at risk for disease progression.

Changes in biophysical properties of individual immune cell populations are directly linked to cytoskeletal reorganization and may reflect the activation of the respective immune cells (14,19,37). Biophysical adaptation is required for leukocyte activation to facilitate margination, extravasation, and migration along chemotactic gradients (19,38,39). Indeed, we demonstrated that the biophysical properties of monocytes, which are key cellular players in the pathogenesis of SSc that drive both inflammation and fibrotic tissue remodeling (e.g., by secreting proinflammatory and profibrotic cytokines, such as IL-6 and TGFβ), are associated with clinical outcomes in SSc patients (2). The changes in biophysical properties of circulating monocytes in SSc patients with extensive, progressive ILD were partially reproduced in vitro by exposure of healthy monocytes to TGFβ or to serum from SSc patients with extensive, progressive ILD, suggesting that a profibrotic environment with high levels of TGFβ and/or SSc-specific autoantibodies might play a direct role in inducing these changes.

We demonstrated that monocytes had different biophysical changes in different clinical subsets of SSc patients: 1) a higher median cross-sectional area, a higher deformation, and reduced heterogeneity of area in SSc patients with active disease or with severe skin or lung involvement; 2) a reduced heterogeneity of deformation in SSc patients with extensive ILD or progressive skin or lung involvement; and 3) an increased stiffness (intra-donor median of Young's modulus) in SSc patients with progressive ILD or with PAH. The increase in cell area and deformation might directly reflect their pathologic activation; an increased area might slow the monocyte flow through capillaries and thus facilitate their margination and promote their extravasation into affected tissues (further facilitated by their higher deformation) (38,40). Indeed, monocytes from SSc patients have been reported to have increased migratory, chemotactic, and adhesive capacity (3). The reduced intra-donor heterogeneity of area or deformation of monocytes might reflect a loss of homeostatic or antifibrotic/antiinflammatory subpopulations of monocytes with lower area or deformation in SSc patients with active or severe disease. However, these hypotheses require further experimental validation.

In SSc patients with worsening of skin or lung involvement at the time of measurement, monocyte subsets had a lower intra-donor heterogeneity of deformation. The intra-donor heterogeneity of deformation of monocytes also decreased with the severity of skin or lung involvement. Moreover, intermediate monocytes had a lower SD_{ID} of deformation in patients with future ILD progression at a follow-up visit 1 year after the measurements, and the SD_{ID} of deformation of monocyte subsets did not correlate with disease activity. Together, these findings indicate that monocytes of SSc patients with severe disease have a lower intra-donor heterogeneity of deformation early in the disease course, and this property is maintained during disease progression. Changes in the SD_{ID} of deformation of monocytes might thus serve as an early marker for patients at high risk for severe, progressive disease. This change can be reproduced in vitro by exposure of healthy monocytes to serum of patients with extensive, progressive ILD, but not by exposure to TGFβ or IL-6, suggesting that disease-specific serum factors with temporal stability, such as the presence of anti–topoisomerase I autoantibodies, might contribute to the reduced heterogeneity of deformation of monocytes. However, this biophysical alteration is associated with the extent or progression of ILD after adjusting for autoantibody status, and thus provides more information than simple risk stratification by autoantibody status.

In contrast to changes in the SD_{ID} of deformation, the stiffness of monocyte subsets (measured by Young's modulus) was higher only in SSc patients with ILD progression at the time of analyses, but not in patients with severe skin or lung involvement. This change can be reproduced in vitro by exposure of healthy monocytes to both TGFβ and to serum from patients with extensive, progressive ILD, suggesting that a profibrotic environment with high levels of TGFβ might be responsible at least in part for the increased stiffness of circulating monocytes in SSc patients. An increase in monocyte stiffness might thus indicate active lung remodeling rather than the presence of damage. This might be of particular interest, since evaluation of active lung remodeling in SSc remains challenging with current tools, due in part to the confounding effects of irreversible tissue damage (41). Further studies with long-term follow-up and higher numbers of patients are required to confirm these hypotheses.

Of note, changes in the biophysical properties of circulating cells can influence the flow of blood through capillaries (42–44). This might be of particular relevance in SSc, since changes in blood flow contribute to ischemia in the context of preexisting vascular abnormalities in SSc (45). In line with this, we observed that inflammatory monocytes have an increased area in patients with active digital ulcerations, whereas intermediate monocytes are stiffer in patients with PAH (Supplementary Tables 14 and 15, http://onlinelibrary.wiley.com/doi/10.1002/art.42394). Since

these changes were not observed in patients with AAV, they reflect SSc-specific abnormalities rather than general vascular pathology. An increase in either area or stiffness of monocytes could, in theory, lead to an increased retention of inflammatory monocytes in capillaries with reduced blood flow.

Our study had certain limitations. First, this study predominantly included patients of German ethnicity. Further studies will be required to confirm our findings in additional cohorts that include patients with different ethnicities. Second, the follow-up time was limited to up to 1 year after the RT-FDC measurements were made, and the number of patients with progression of skin or lung involvement within this timeframe was limited. Additional studies may provide longer clinical follow-up on larger cohorts to determine potential associations with event-driven outcomes such as new organ involvement, hospitalization, or survival. Third, regarding treatment, we only stratified patients according to whether or not they received immunosuppressive therapy, but not by drug class. Such an analysis would require larger cohorts, may allow for the evaluation of whether current therapeutic interventions revert the aberrant biophysical properties of monocytes, and may reveal whether clinical response to treatment can be predicted by RT-FDC–based phenotyping of monocytes. Finally, characterization of the molecular mechanisms underlying the observed biophysical alterations will require further studies based on enrichment of cells with different biophysical states, with subsequent "omic" analyses such as single-cell RNA sequencing or mass cytometry (46). This approach could provide candidates for therapeutic interventions in SSc that target the biophysical alterations of circulating monocytes.

Biophysical phenotyping of immune cells provides access to a mostly unexplored layer of information with direct relevance for the immune cell activation state. RT-FDC–based biophysical phenotyping can be performed with high-throughput and minimal costs, which facilitates its use in a clinical context. Many biomarker candidates proposed for the diagnosis or outcome evaluation of SSc or other fibrotic diseases such as gene signatures or panels of multiple cytokines are not currently used in routine clinical assessment, as they are too expensive and/or labor intensive (47,48). Thus, RT-FDC–based biophysical phenotyping of circulating monocytes has the potential to address a yet to be fulfilled need for biomarkers that directly reflect pathophysiologic processes in SSc and other fibrotic diseases, after confirmation in additional cohorts.

ACKNOWLEDGMENTS

We thank Wolfgang Espach, Vladyslav Fedorchenko, Lena Summa, Christoph Liebel, and Regina Kleinlein for their excellent technical assistance. Open Access funding enabled and organized by Projekt DEAL.

AUTHOR CONTRIBUTIONS

All authors were involved in drafting the article or revising it critically for important intellectual content, and all authors approved the final version to be published. Dr. Matei had full access to all of the data in the study and takes responsibility for the integrity of the data and the accuracy of the data analysis.

Study conception and design. Matei, Györfi, Schett, Distler.

Acquisition of data. Matei, Kubánková, Xu, Boxberger, Soteriou, Papava, Prater, Hong.

Analysis and interpretation of data. Matei, Kubánková, Xu, Györfi, Boxberger, Papava, Prater, Hong, Bergmann, Kräter, Schett, Guck, Distler.

REFERENCES

1. Wynn TA. Cellular and molecular mechanisms of fibrosis. J Pathol 2008;214:199–210.
2. Distler JH, Gyorfi AH, Ramanujam M, et al. Shared and distinct mechanisms of fibrosis [review]. Nat Rev Rheumatol 2019;15:705–30.
3. Kania G, Rudnik M, Distler O. Involvement of the myeloid cell compartment in fibrogenesis and systemic sclerosis [review]. Nat Rev Rheumatol 2019;15:288–302.
4. Carvalheiro T, Zimmermann M, Radstake T, et al. Novel insights into dendritic cells in the pathogenesis of systemic sclerosis. Clin Exp Immunol 2020;201:25–33.
5. Ross RL, Corinaldesi C, Migneco G, et al. Targeting human plasmacytoid dendritic cells through BDCA2 prevents skin inflammation and fibrosis in a novel xenotransplant mouse model of scleroderma. Ann Rheum Dis 2021;80:920–9.
6. O'Reilly S, Hugle T, van Laar JM. T cells in systemic sclerosis: a reappraisal. Rheumatology (Oxford) 2012;51:1540–9.
7. Chizzolini C. T cells, B cells, and polarized immune response in the pathogenesis of fibrosis and systemic sclerosis. Curr Opin Rheumatol 2008;20:707–12.
8. Benyamine A, Magalon J, Sabatier F, et al. Natural killer cells exhibit a peculiar phenotypic profile in systemic sclerosis and are potent inducers of endothelial microparticles release. Front Immunol 2018;9:1665.
9. Pecher AC, Kettemann F, Asteriti E, et al. Invariant natural killer T cells are functionally impaired in patients with systemic sclerosis. Arthritis Res Ther 2019;21:212.
10. Paleja B, Low AH, Kumar P, et al. Systemic sclerosis perturbs the architecture of the immunome. Front Immunol 2020;11:1602.
11. Di Carlo D. A mechanical biomarker of cell state in medicine. J Lab Autom 2012;17:32–42.
12. Guck J, Chilvers ER. Mechanics meets medicine. Sci Transl Med 2013;5:212fs41.
13. Bougen-Zhukov N, Loh SY, Lee HK, et al. Large-scale image-based screening and profiling of cellular phenotypes. Cytometry A 2017;91:115–25.
14. Bufi N, Saitakis M, Dogniaux S, et al. Human primary immune cells exhibit distinct mechanical properties that are modified by inflammation. Biophys J 2015;108:2181–90.
15. Ekpenyong AE, Whyte G, Chalut K, et al. Viscoelastic properties of differentiating blood cells are fate- and function-dependent. PLoS One 2012;7:e45237.
16. Urbanska M, Winzi M, Neumann K, et al. Single-cell mechanical phenotype is an intrinsic marker of reprogramming and differentiation along the mouse neural lineage. Development 2017;144:4313–21.
17. Bashant KR, Vassallo A, Herold C, et al. Real-time deformability cytometry reveals sequential contraction and expansion during neutrophil priming. J Leukoc Biol 2019;105:1143–53.
18. Lautenschlager F, Paschke S, Schinkinger S, et al. The regulatory role of cell mechanics for migration of differentiating myeloid cells. Proc Natl Acad Sci U S A 2009;106:15696–701.

19. Bashant KR, Toepfner N, Day CJ, et al. The mechanics of myeloid cells. Biol Cell 2020;112:103–12.
20. Toepfner N, Herold C, Otto O, et al. Detection of human disease conditions by single-cell morpho-rheological phenotyping of blood. Elife 2018;7:e29213.
21. Kubankova M, Hohberger B, Hoffmanns J, et al. Physical phenotype of blood cells is altered in COVID-19. Biophys J 2021;120:2838–47.
22. Tse HT, Gossett DR, Moon YS, et al. Quantitative diagnosis of malignant pleural effusions by single-cell mechanophenotyping. Sci Transl Med 2013;5:212ra163.
23. Rosendahl P, Plak K, Jacobi A, et al. Real-time fluorescence and deformability cytometry. Nat Methods 2018;15:355–8.
24. Otto O, Rosendahl P, Mietke A, et al. Real-time deformability cytometry: on-the-fly cell mechanical phenotyping. Nat Methods 2015;12: 199–202.
25. Herbig M, Krater M, Plak K, et al. Real-time deformability cytometry: label-free functional characterization of cells. Methods Mol Biol 2018; 1678:347–69.
26. Urbanska M, Rosendahl P, Krater M, et al. High-throughput single-cell mechanical phenotyping with real-time deformability cytometry. Methods Cell Biol 2018;147:175–98.
27. Krijgsman D, de Vries NL, Skovbo A, et al. Characterization of circulating T-, NK-, and NKT cell subsets in patients with colorectal cancer: the peripheral blood immune cell profile. Cancer Immunol Immunother 2019;68:1011–24.
28. Tang Y, Li X, Wang M, et al. Increased numbers of NK cells, NKT-like cells, and NK inhibitory receptors in peripheral blood of patients with chronic obstructive pulmonary disease. Clin Dev Immunol 2013; 2013:721782.
29. Abeles D, McPhail MJ, Sowter D, et al. CD14, CD16 and HLA-DR reliably identifies human monocytes and their subsets in the context of pathologically reduced HLA-DR expression by CD14hi/CD16neg monocytes: expansion of CD14hi/CD16pos and contraction of CD14lo/CD16pos monocytes in acute liver failure. Cytometry Part A 2012;81A:823–34.
30. Valentini G, Iudici M, Walker UA, et al. The European Scleroderma Trials and Research group (EUSTAR) task force for the development of revised activity criteria for systemic sclerosis: derivation and validation of a preliminarily revised EUSTAR activity index. Ann Rheum Dis 2017; 76:270–6.
31. Clements PJ, Lachenbruch PA, Ng SC, et al. Skin score: a semiquantitative measure of cutaneous involvement that improves prediction of prognosis in systemic sclerosis. Arthritis Rheum 1990;33:1256–63.
32. Goh NS, Desai SR, Veeraraghavan S, et al. Interstitial lung disease in systemic sclerosis: a simple staging system. Am J Respir Crit Care Med 2008;177:1248–54.
33. Flaherty KR, Wells AU, Cottin V, et al. Nintedanib in progressive fibrosing interstitial lung diseases. N Engl J Med 2019;381:1718–27.
34. Gyorfi AH, Matei AE, Distler JH. Targeting TGF-β signaling for the treatment of fibrosis. Matrix Biol 2018;68–69:8–27.
35. Mihara M, Hashizume M, Yoshida H, et al. IL-6/IL-6 receptor system and its role in physiological and pathological conditions. Clin Sci (Lond) 2012;122:143–59.
36. Scott MK, Quinn K, Li Q, et al. Increased monocyte count as a cellular biomarker for poor outcomes in fibrotic diseases: a retrospective, multicentre cohort study. Lancet Respir Med 2019;7:497–508.
37. Fletcher DA, Mullins RD. Cell mechanics and the cytoskeleton. Nature 2010;463:485–92.
38. Fay ME, Myers DR, Kumar A, et al. Cellular softening mediates leukocyte demargination and trafficking, thereby increasing clinical blood counts. Proc Natl Acad Sci U S A 2016;113:1987–92.
39. Yoshida K, Kondo R, Wang Q, et al. Neutrophil cytoskeletal rearrangements during capillary sequestration in bacterial pneumonia in rats. Am J Respir Crit Care Med 2006;174:689–98.
40. Dewitt S, Francis RJ, Hallett MB. Ca(+) and calpain control membrane expansion during the rapid cell spreading of neutrophils. J Cell Sci 2013;126:4627–35.
41. Bergmann C, Distler JH, Treutlein C, et al. 68Ga-FAPI-04 PET-CT for molecular assessment of fibroblast activation and risk evaluation in systemic sclerosis-associated interstitial lung disease: a single-centre, pilot study. Lancet Rheumatol 2021;3:e185–94.
42. Rosenbluth MJ, Lam WA, Fletcher DA. Analyzing cell mechanics in hematologic diseases with microfluidic biophysical flow cytometry. Lab Chip 2008;8:1062–70.
43. Qiu Y, Myers DR, Lam WA. The biophysics and mechanics of blood from a materials perspective [review]. Nat Rev Mater 2019;4: 294–311.
44. Tietze S, Krater M, Jacobi A, et al. Spheroid culture of mesenchymal stromal cells results in morphorheological properties appropriate for improved microcirculation. Adv Sci (Weinh) 2019;6:1802104.
45. Matucci-Cerinic M, Kahaleh B, Wigley FM. Evidence that systemic sclerosis is a vascular disease [review]. Arthritis Rheum 2013;65: 1953–62.
46. Nawaz AA, Urbanska M, Herbig M, et al. Intelligent image-based deformation-assisted cell sorting with molecular specificity. Nat Methods 2020;17:595–9.
47. Skaug B, Assassi S. Biomarkers in systemic sclerosis. Curr Opin Rheumatol 2019;31:595–602.
48. Affandi AJ, Radstake TR, Marut W. Update on biomarkers in systemic sclerosis: tools for diagnosis and treatment. Semin Immunopathol 2015;37:475–87.